Biochimica et Biophysica Acta 1837 (2014) 1739–1747

Contents lists available at ScienceDirect

Biochimica et Biophysica Acta

journal homepage: www.elsevier.com/locate/bbabio

A short-chain alkyl derivative of Rhodamine 19 acts as a mild uncoupler of mitochondria and a neuroprotector

Ljudmila S. Khailova [a,b], Denis N. Silachev [a,b], Tatyana I. Rokitskaya [a,b], Armine V. Avetisyan [a,b], Konstantin G. Lyamsaev [a,b], Inna I. Severina [a,b], Tatyana M. Il'yasova [a,b], Mikhail V. Gulyaev [d], Vera I. Dedukhova [a,b], Tatyana A. Trendeleva [e], Egor Y. Plotnikov [a,b], Renata A. Zvyagilskaya [b,e], Boris V. Chernyak [a,b], Dmitry B. Zorov [a,b], Yuri N. Antonenko [a,b,*], Vladimir P. Skulachev [a,b,c,*]

[a] Lomonosov Moscow State University, Belozersky Institute of Physico-Chemical Biology, Vorobyevy Gory 1, Moscow 119991, Russia
[b] Lomonosov Moscow State University, Institute of Mitoengineering, Vorobyevy Gory 1, Moscow 119991, Russia
[c] Lomonosov Moscow State University, Faculty of Bioengineering and Bioinformatics, Vorobyevy Gory 1, Moscow 119991, Russia
[d] Lomonosov Moscow State University, Faculty of Fundamental Medicine, Lomonosovsky Prospect 31/5, Moscow 117192, Russia
[e] A. N. Bach Institute of Biochemistry, Russian Academy of Sciences, Leninsky Prospect 33/2, 119071 Moscow, Russia

ARTICLE INFO

Article history:
Received 25 March 2014
Received in revised form 20 June 2014
Accepted 9 July 2014
Available online 16 July 2014

Keywords:
Mitochondria
Mild uncoupler
Protonophore
Rhodamine
Membrane potential

ABSTRACT

Limited uncoupling of oxidative phosphorylation is known to be beneficial in various laboratory models of diseases. The search for cationic uncouplers is promising as their protonophorous effect is self-limiting because these uncouplers lower membrane potential which is the driving force for their accumulation in mitochondria. In this work, the penetrating cation Rhodamine 19 butyl ester (C_4R1) was found to decrease membrane potential and to stimulate respiration of mitochondria, appearing to be a stronger uncoupler than its more hydrophobic analog Rhodamine 19 dodecyl ester ($C_{12}R1$). Surprisingly, $C_{12}R1$ increased H^+ conductance of artificial bilayer lipid membranes or induced mitochondria swelling in potassium acetate with valinomycin at concentrations lower than C_4R1. This paradox might be explained by involvement of mitochondrial proteins in the uncoupling action of C_4R1. In experiments with HeLa cells, C_4R1 rapidly and selectively accumulated in mitochondria and stimulated oligomycin-sensitive respiration as a mild uncoupler. C_4R1 was effective in preventing oxidative stress induced by brain ischemia and reperfusion in rats: it suppressed stroke-induced brain swelling and prevented the decline in neurological status more effectively than $C_{12}R1$. Thus, C_4R1 seems to be a promising example of a mild uncoupler efficient in treatment of brain pathologies related to oxidative stress.

1. Introduction

Protection against oxidative stress-related diseases exerted by protonophorous uncouplers is generally associated with their ability to reduce ROS production by lowering mitochondrial membrane potential ($\Delta\psi$) [1,2]. However, high uncoupler concentrations lead to an arrest of ATP production and impairment of the vitally important ATP-dependent biochemical reactions. The dependence of ATP production on the value of proton motive force is very steep, providing a "window" between protective and toxic concentrations of an uncoupler. There is an opinion that this window is quite wide considering that ATP synthase activity reaches its maximum at rather low $\Delta\psi$ (100–120 mV, [3–5]) and all values above these are redundant stimulating leak and hyperbolically inducing ROS generation in mitochondria [1,6]. Modest ("mild") uncoupling is the fall of the membrane potential within this safe window, thus retaining oxidative phosphorylation, while causing a significant drop in the proton leak and the ROS level [6,7]. Even a small decrease in $\Delta\psi$ initially exceeding the level of approximately 150 mV was shown to disproportionately decrease H_2O_2 generation by mitochondria [6–9]. The mild uncoupling phenomenon was suggested to occur in animal cells containing mitochondrial uncoupling proteins (UCPs) performing two functions, i.e. heat generation and protection against oxidative injury [10]. According to [11–14], uncoupling proteins, such as UCP2, play an essential role in protection against

Abbreviations: $\Delta\psi$, transmembrane electric potential difference; BLM, bilayer lipid membrane; BSA, bovine serum albumin; C_2R1, Rhodamine 19 ethyl ester or Rhodamine 6G; C_4R1, Rhodamine 19 butyl ester; C_4R4, Rhodamine B butyl ester; C_8R1, Rhodamine 19 octyl ester; $C_{10}R1$, Rhodamine 19 decyl ester; $C_{12}R1$, Rhodamine 19 dodecyl ester; $C_{16}R1$, Rhodamine 19 octadecyl ester; CCCP, carbonyl cyanide *m*-chlorophenylhydrazone; DPhPC, diphytanoylphosphatidylcholine; DNP, 2,4-dinitrophenol; DiSC3-(5), 3,3′-dipropylthiadicarbocyanine iodide; FCCP, carbonyl cyanide-*p*-trifluoromethoxyphenylhydrazone; FCS, fluorescence correlation spectroscopy; MCAO, middle cerebral artery occlusion; MR, magnetic resonance; MRI, magnetic resonance imaging; PBS, phosphate buffered saline; PIA, peak intensity analysis; ROS, reactive oxygen species; TMRE, tetramethylrhodamine ethyl ester; TIRF, total internal reflection fluorescence

* Corresponding authors at: Belozersky Institute of Physico-Chemical Biology, Moscow State University, Moscow 119991, Russia. Tel.: +7 495 939 51 49; fax: +7 495 939 31 81.
E-mail addresses: antonen@genebee.msu.ru (Y.N. Antonenko), skulach@belozersky.msu.ru (V.P. Skulachev).

http://dx.doi.org/10.1016/j.bbabio.2014.07.006
0005-2728/

neurodegenerative diseases (cerebral ischemia, traumatic brain injury (TBI), and Parkinson's disease).

Stroke is a major cause of death and disability, and it is imperative to develop therapeutics to mitigate stroke-related injury. It is known that cell injury and neuronal death after oxidative stress, including ischemia/reperfusion of brain, involve structural and functional abnormalities in mitochondria [15]. In view of the above-mentioned relationship between membrane potential and ROS production in mitochondria, the neuroprotective effects of conventional uncouplers such as 2,4-dinitrophenol (DNP) administered in post-reperfusion period in a stroke model can be easily explained by tightly coupled changes of these two functions [16]. However, known uncouplers used in the *in vivo* studies are toxic thus stimulating the search of those uncouplers which the living organisms can tolerate.

We have shown in our previous work that long-chain alkyl derivatives of Rhodamine 19 at micromolar concentrations uncouple mitochondria by inducing proton fluxes through their inner membrane [17]. Importantly, as to induced proton transfer, analogs of Rhodamine B (e.g. C_4R4) were inactive due to the presence of additional ethyl groups, which hinder protonation of one of two nitrogen atoms of the rhodamine moiety (for chemical structures, see Fig. S1). We have also reported that C_4R1 does not carry protons across liposomal membranes [17]. In the present study, we show that C_4R1 uncouples rat liver mitochondria even more effectively than the corresponding long-chain Rhodamine 19 derivatives. We suggest that, similarly to fatty acids that uncouple mitochondria in an ADP/ATP-antiporter-mediated fashion [18], C_4R1 can uncouple via an interaction with some protein(s) of the mitochondrial inner membrane. In our previous studies, we demonstrated that the mitochondria-targeted uncoupler $C_{12}R1$ exerts significant nephroprotection under ischemia/reperfusion of the kidney, as well as under rhabdomyolysis as inferred from less expressed renal dysfunction judged by elevated level of blood creatinine and urea. Similar nephroprotective properties were observed for low doses of DNP [19]. In this study, we compared the potency of two Rhodamine 19 derivatives (C_4R1 and $C_{12}R1$) as protective agents in brain ischemia and reperfusion. Our results can be relevant to the search for substances causing mild uncoupling of mitochondria, which are considered to be a promising therapeutic strategy to treat a number of pathologies [2,20,21].

2. Materials and methods

2.1. Materials

Derivatives of rhodamine were synthesized in our institute by Natalia V. Sumbatyan and Galina A. Korshunova as described in [22,23]. Sucrose was from ICN, Rhodamine 6G was from Fluka, and TMRE and 3,3′-dipropylthiadicarbocyanine iodide ($DiSC_3$-(5)) were from Molecular Probes. Diphytanoylphosphatidylcholine (DPhPC) was from Avanti Polar Lipids. Other chemicals were from Sigma-Aldrich.

2.2. Planar phospholipid bilayers

Bilayer lipid membrane (BLM) was formed from 2% decane solution of DPhPC on a 0.6-mm aperture in a Teflon septum separating the experimental chamber into two compartments of equal size (volumes, 3 ml). Electrical parameters were measured with two AgCl electrodes placed into the solutions on the two sides of the BLM via agar bridges, using a Keithley 6517 amplifier (Cleveland, Ohio, USA). The incubation mixture contained 50 mM Tris–HCl and 50 mM KCl, pH 7.0.

2.3. Isolation of rat liver mitochondria

Rat liver mitochondria were isolated by differential centrifugation [24] in medium containing 250 mM sucrose, 5 mM MOPS, 1 mM EGTA, and bovine serum albumin (0.5 mg/ml), pH 7.4. The final washing was performed in medium of the same composition. Protein concentration was determined using the biuret method. Handling of animals and experimental procedures with them were conducted in accordance with the international guidelines for animal care and use and were approved by the Institutional Ethics Committee of Belozersky Institute of Physico-Chemical Biology at Moscow State University.

2.4. Mitochondrial respiration

Respiration of isolated mitochondria was measured using a standard polarographic technique with a Clark-type oxygen electrode (Strathkelvin Instruments, UK) at 25 °C using the 782 system software. The incubation medium contained 250 mM sucrose, 5 mM MOPS, and 1 mM EGTA, pH 7.4. The mitochondrial protein concentration was 0.8 mg/ml. Oxygen uptake is expressed as nmol/min mg protein.

2.5. Mitochondrial membrane potential measurement

DiSC3-(5) was used as a membrane potential probe [25]. Fluorescence intensity at 690 nm (excitation at 622 nm) was measured with a Panorama Fluorat 02 spectrofluorimeter (Lumex, Russia). The medium for measurements contained 250 mM sucrose, 20 mM MOPS, 1 mM EDTA, 5 mM succinate, 1 μM rotenone, and 1 μM DiSC3-(5), pH 7.4. The mitochondrial protein concentration was 0.4 mg/ml.

2.6. Swelling of mitochondria in potassium acetate

The protonophoric ability of rhodamine derivatives was tested by induction of swelling of non-respiring rat liver mitochondria incubated in buffered isotonic potassium acetate in the presence of valinomycin. Under these conditions, mitochondria do not swell because acetate can cross the membrane only as undissociated acetic acid, and the transmembrane passage of potassium in the form of the K^+–valinomycin complex generates a charge imbalance ($\Delta\psi$), preventing further permeation of K^+ [26]. Intramitochondrial accumulation of potassium acetate becomes possible only if H^+ is exported from the inner compartment of mitochondria, thus discharging $\Delta\psi$ which limits the swelling. This H^+ export process can be mediated, for example, by synthetic protonophores [27]. Swelling of mitochondria was recorded as the decrease in absorbance at 600 nm or 540 nm. Briefly, an aliquot of mitochondria (0.5 mg mitochondrial protein) was added to 1 ml of the "swelling medium" containing 145 mM potassium acetate, 5 mM Tris, 0.5 mM EDTA, 3 μM valinomycin, 1 μM rotenone, pH 7.4.

2.7. Yeast mitochondria

In this study, we used the *Yarrowia lipolytica* yeast, an obligate aerobe. The strain was obtained by one of us (R.A.Z.) as a pure isolate from epiphytic microflora of salt-excreting leaves of arid plants (Negev Desert, Israel) and identified as an anamorph of *Y. lipolytica* (Wick.) van der Walt and Arx. The yeast cells were routinely grown at 28 °C in agitated (220 rpm) succinate-containing semi-synthetic medium to the late exponential growth phase (OD_{590} = 3.4–3.6). Mitochondria from *Y. lipolytica* cells were prepared as described previously (38). They were fully active for at least 4 h when kept on ice. Oxygen consumption by mitochondria was monitored amperometrically at room temperature, using the Clark-type oxygen electrode. The incubation medium contained 0.6 M mannitol, 20 mM Tris–pyruvate, 5 mM Tri-–malate, 0.5 mM EGTA, 0.2 mM Tris–phosphate, pH 7.2–7.4, and mitochondria (0.5 mg protein per ml). Mitochondrial protein was determined using the Bradford method (Bradford, 1976) with BSA as the standard.

2.8. FCS experimental setup

Rhodamine uptake by isolated mitochondria was measured by fluorescence correlation spectroscopy (FCS). Peak intensity analysis (PIA) records fluorescence time traces of suspensions of dye-doped

mitochondria, representing sequences of peaks of different intensity reflecting their random walk through the confocal volume [28]. The experimental data were obtained under stirring, which increased the number of events by about three orders of magnitude, thus substantially enhancing the resolution of the method. The setup of our own construction was described previously [28]. Briefly, fluorescence excitation and detection were provided by a Nd:YAG solid state laser with a 532-nm beam, attached to an Olympus IMT-2 epifluorescence inverted microscope equipped with a 40×, NA 1.2 water immersion objective (Carl Zeiss, Jena, Germany). The fluorescence passed through an appropriate dichroic beam splitter and a long-pass filter and was imaged onto a 50-μm core fiber coupled to an avalanche photodiode (SPCM-AQR-13-FC, Perkin Elmer Optoelectronics, Vaudreuil, Quebec, Canada). The output signal $F(t)$ was sent to a personal computer, using a fast interface card (Flex02-01D/C, Correlator.com, Bridgewater, NJ). The signal was measured in Hz, i.e. number of photons per second. The data acquisition time T was 30 s. The card generated the autocorrelation function of the signal $G(\tau)$ defined as

$$G(\tau) = \frac{1}{T}\int_0^T F(t)F(t+\tau)dt = <F(t+\tau)F(t)>$$

2.9. Cultivation of HeLa cells

HeLa cells were cultivated in DMEM with 10% fetal bovine serum (FBS) and harvested at 70–80% confluency. The cells were washed and suspended in DMEM without the serum just before measurements. The final cell concentration in the polarographic chamber was 4–5 10^6 cells/ml. The protein concentration was determined according to the Lowry protein assay. Oxygen consumption was recorded at 37 °C as described above.

2.10. Cytofluorimetry of HeLa cells

The HeLa cells were cultivated in DMEM with 10% FBS and 100 nM of a rhodamine compound. The cells were harvested and analyzed using fluorescent flow cytometry (Beckman-Coulter FC-500). The Rhodamine was washed out after 45 min incubation, and the measurement was continued. Where indicated, 10 μM FCCP was added 30 min before the Rhodamine.

2.11. Microscopy

HeLa cells were incubated with 100 nM C_4R1 or $C_{12}R1$ and analyzed without washing out of the fluorescent compound using a pseudo total internal reflection fluorescence (pseudo-TIRF) microscope built upon an inverted microscope (Nikon Eclipse Ti-E) equipped with a TIRF objective (Nikon 60×, 1.27 WI). Z-stacks with a step of 0.3 μm were obtained.

2.12. Middle cerebral artery occlusion model of focal ischemia

Middle cerebral artery occlusion (MCAO) surgery and the sham operation were performed as previously described [29]. Briefly, rats were anesthetized with i/p injection of 300 mg/kg chloral hydrate. The right common carotid artery was exposed through a midline cervical incision. A heparinized intraluminal silicon-coated monofilament (diameter, 0.25 mm) was introduced via the external carotid artery into the internal carotid artery to occlude the blood supply to the middle cerebral artery region. A feedback-controlled heating pad supplemented with an infrared lamp was used to maintain core temperature (37.0 ± 0.5 °C) during ischemia. After 60 min of occlusion, the filament was gently pulled out and the external carotid artery was permanently closed by cauterization. In sham-operated rats, the right common carotid artery was exposed and the external carotid artery was electrocoagulated without introducing the filament into the internal carotid artery. C_4R1 and $C_{12}R1$ at dose 1 μmol/kg was i/p injected immediately after the beginning of reperfusion. The rats were randomly divided into the following groups: (1) SHAM + VEHICLE ($n = 6$), (2) MCAO + VEHICLE ($n = 7$), (3) MCAO + C_4R1 ($n = 6$), (4) MCAO + $C_{12}R1$ ($n = 6$). Infarct volume was quantified by analyzing brain MRI images obtained 24 h after the MCAO as described previously [29]. Brain swelling was also measured in the MRI images and calculated using the formula: swelling (edema) = (volume of right hemisphere − volume of left hemisphere)/volume of left hemisphere [30]. Ischemically damaged volume for each group was normalized to the mean for the group MCAO + VEHICLE.

2.13. Limb-placing test

The modified version of the limb-placing test consisting of seven tasks was used to assess forelimb and hindlimb responses to tactile and proprioceptive stimulation [31]. The rats were habituated for handling and tested before operation and after the reperfusion for 24 h. For each task, the following scores were used: 2 points, normal response; 1 point, delayed and/or incomplete response; and 0 points, no response. Over seven tasks, the mean score was evaluated.

2.14. Analysis of C_4R1 accumulation in kidney and brain

Rats were injected i/p with 1 μmol C_4R1/kg. After 3 h, the kidney and brain were excised, fixed with 4% formaldehyde in PBS, and sliced using a VibroSlice microtome (World Precision Instruments, USA) into 100 μm thick sections. Slices were imaged with an LSM510 inverted confocal microscope (Carl Zeiss Inc., Jena, Germany) with excitation at 543 nm and emission at 560–590 nm. As a negative control, organs from untreated animals were used.

2.15. Statistics

Statistical analyses were performed using STATISTICA 7.0 for Windows (StatSoft, Inc.). All data are presented as means ± standard error of means (SEM). Variance homogeneity was assessed with Levene's test. Statistical differences between groups in the data of infarct volume and brain swelling were analyzed using one-way ANOVA with Tukey's post-hoc test. Statistical differences in the limb-placing tests between groups were analyzed using the Kruskal–Wallis test with the Mann–Whitney u-test (the Bonferroni post-hoc correction was applied). Values for $p < 0.05$ were assumed to be statistically significant.

3. Results

Our previous finding of the uncoupling activity of mitochondria-targeted alkyl rhodamine derivatives [17] pointed to their possible protective action against oxidative stress-related diseases. Actually, $C_{12}R1$ proved to be an effective nephroprotector and neuroprotector under kidney and brain ischemia/reperfusion [19]. To examine the relationship between the anti-oxidative defense exerted by alkyl rhodamine derivatives and their lipophilicity-dependent uncoupling activity, we choose the model of MCAO focal ischemia as optimal for evaluation of the infarct size having low variability [32]. After exposure of the rat brain to MCAO we observed an extensive cortical and striatal damage with remarkable brain edema. We examined the effects of i/p injections of C_4R1 or $C_{12}R1$ on ischemic brain injury of rat after their administration immediately after restoration of the blood flow to the brain. The treatment with C_4R1 diminished brain swelling almost four fold (from 20 ± 2% to 5.2 ± 1.9%, $p < 0.05$), while the protective effect of $C_{12}R1$ was not so remarkable but still significantly decreasing the swelling two fold to 10.4 ± 0.9% ($p < 0.05$) (Fig. 1A, B). Apart from this, C_4R1 and $C_{12}R1$ provided partial protection of the brain in the experimental

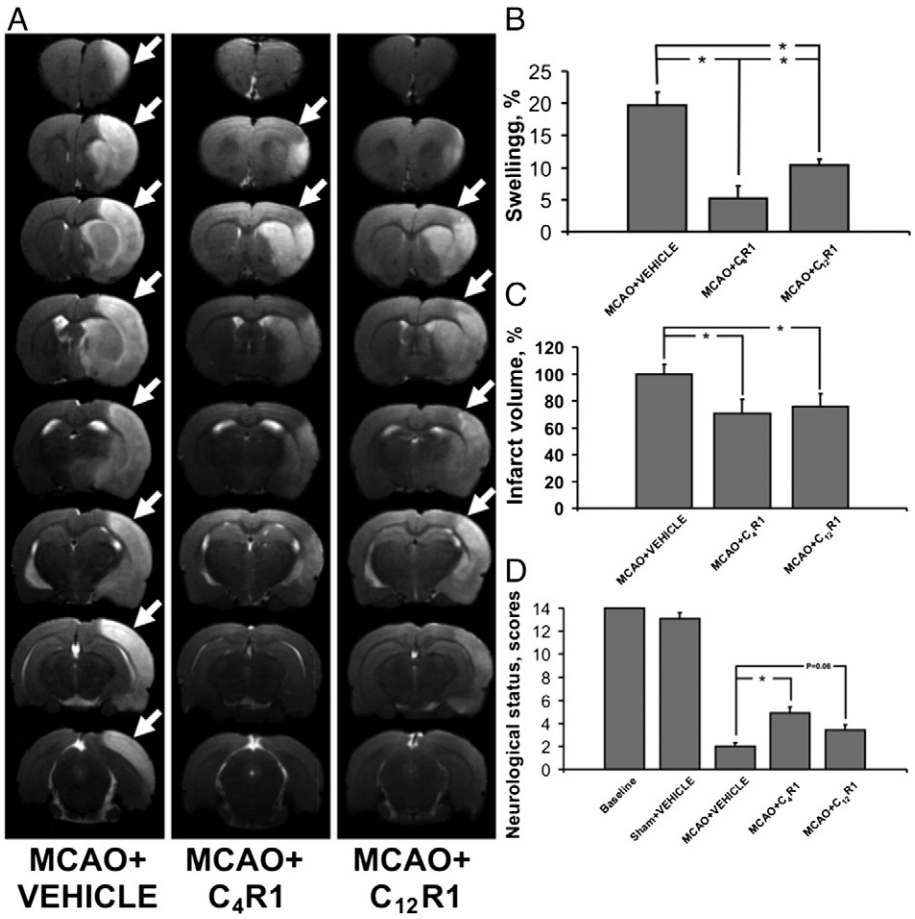

Fig. 1. Protection of ischemia/reperfusion-injured brain by the C_4R1 or $C_{12}R1$ treatment starting immediately after reperfusion. (A) Representative T2-weighted MR-images from coronal brain sections (0.8 mm thick, from rostral (top) towards caudal (bottom)) obtained 24 h after reperfusion. Hyperintensitive regions refer to ischemic areas depicted in the right hemisphere. Arrows point to the more pronounced edema in the section. (B) Brain edema (swelling) and (C) infarct volume were evaluated by using MRI with analysis of T2-weighted images. (D) Neurological deficit scores estimated in the limb-placing test. * Denotes significant difference from the MCAO + VEHICLE or MCAO groups ($p < 0.05$) (One-way ANOVA, followed by Tukey's post-hoc analysis for (B) and (C); Kruskal–Wallis test with the Mann–Whitney *U*-test for (D)).

stroke model, the infarct volume being reduced to 70% and 75% of the control group, respectively ($p < 0.05$) (Fig. 1C). The neurological score after 24 h of reperfusion demonstrates that C_4R1 and $C_{12}R1$ significantly decrease neurological deficit of the ischemic animals. While the intact rats before the induction of ischemia scored 14 in limb-placing test, and sham-operated animals scored 13.1 ± 0.5, in rats exposed to ischemia this index was only 2 ± 0.3. The treatment with C_4R1 and $C_{12}R1$ restored the neurological status to 5 ± 0.5 ($p < 0.05$) and 3.5 ± 0.5, respectively (Fig. 1D). Thus C_4R1, in spite of being much less lipophilic than $C_{12}R1$, exhibited a higher therapeutic effect.

To shed light on the causes of the unexpectedly high protective effect of C_4R1 in living organisms, we performed comparative measurements of the uncoupling activity of C_4R1 and $C_{12}R1$ in isolated mitochondria. We found (Fig. 2A) that C_4R1 stimulated respiration of rat liver mitochondria in State 4 at substantially lower (micromolar) concentrations than $C_{12}R1$ (tens of micromolar). Fig. 2B shows these effects as a function of C_4R1 or $C_{12}R1$ concentration (with succinate as the substrate). The C_{50} values for C_4R1 and $C_{12}R1$ were about 1 μM and 30 μM, respectively. C_4R4 and $C_{12}R4$, which contain no dissociable H^+, were ineffective as uncouplers (data not shown). Their stimulation of respiration supported by glutamate + malate as substrates (curves 1 and 2 of Fig. 2A) was lower than that with succinate (curves 3 and 4 of Fig. 2A). The addition of the conventional strong uncoupler FCCP at the end of the records stimulated respiration with succinate but not with glutamate + malate (Fig. 2A), suggesting an inhibiting effect of an excess of the rhodamine derivatives on the activity of NADH-dehydrogenase which is more sensitive to inhibitory effects of other uncouplers than complex II and III [33,34]. In Fig. 2C, CCCP, C_4R1 and $C_{12}R1$ are compared as stimulators and inhibitors of respiration of yeast mitochondria oxidizing NAD-substrates. It is seen that all three compounds first stimulated respiration and then inhibited it when the uncoupler concentration rose. The window between stimulating and inhibiting concentrations for C_4R1 proved to be as high as 8 times, whereas for $C_{12}R1$ it was less than 3.

The analysis of uncoupling activity of the Rhodamine derivatives as a function of the length of the alkyl chain (substrate, succinate) showed that C_4R1 was the most efficient uncoupler, while a shorter alkyl (C_2R1, i.e. Rhodamine 6G), or longer alkyls (C_8R1, $C_{10}R1$, $C_{12}R1$, $C_{16}R1$) exhibited lower (if any) activity (Fig. 3A). Fig. 3B shows a Rhodamine-mediated decrease in the mitochondrial membrane potential measured with the potential-sensitive dye DiSC3-(5). In the case of $C_{12}R1$, the decrease in the potential was slow and overall less pronounced as compared to C_4R1 (Fig. 3B).

In view of the data on the strong uncoupling activity of C_4R1, the low proton-carrying activity of this compound on lipid vesicles reported in our previous work [17] seems to be controversial. In the present study, we used an alternative approach and measured electric diffusion potential generation on a planar bilayer lipid membrane (BLM), driven by a transmembrane pH gradient. In this system, addition of FCCP resulted in a transmembrane H^+ flux generating an electrical potential difference across the BLM, the more acidic compartment being negatively charged. We found (Fig. 4) that $C_{12}R1$ can effectively substitute for FCCP, whereas C_4R1 was less active. The maximal magnitude of the generated potential was close to the theoretical (Nernstian) limit

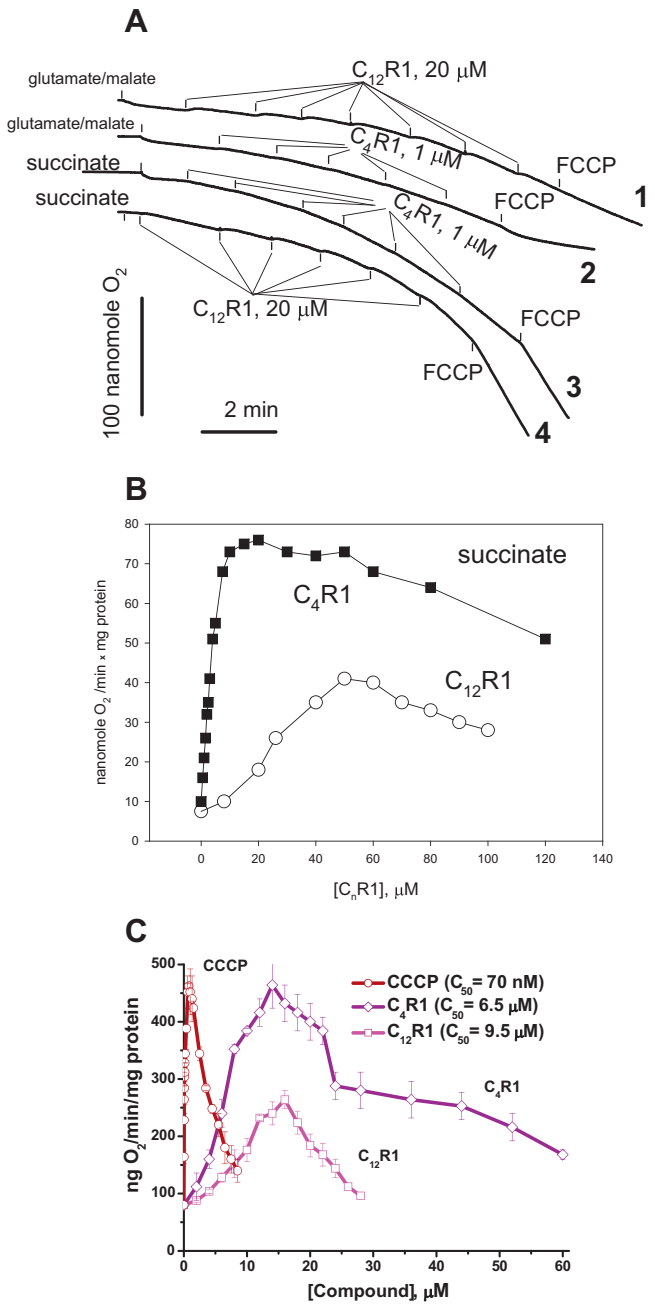

Fig. 2. A. Stimulation of respiration of rat liver mitochondria by C_4R1 and $C_{12}R1$. In samples with succinate, the medium was supplemented with 2 μM rotenone. Additions where indicated: 5 mM succinate, 4 mM glutamate + 1 mM malate, 1 μM C_4R1, 20 μM $C_{12}R1$, 0.1 μM FCCP. B. Dose dependence of stimulation of succinate oxidation by C_4R1 and $C_{12}R1$. C. Effect of CCCP, C_4R1 and $C_{12}R1$ on the oxygen consumption by *Yarrowia lipolytica* mitochondria in State 4. Incubation medium contained 0.6 M mannitol, 20 mM Tris–pyruvate, 5 mM Tris–malate, 0.5 mM EGTA, 0.2 mM Tris–phosphate, pH 7.2, and mitochondria (0.5 mg protein/ml).

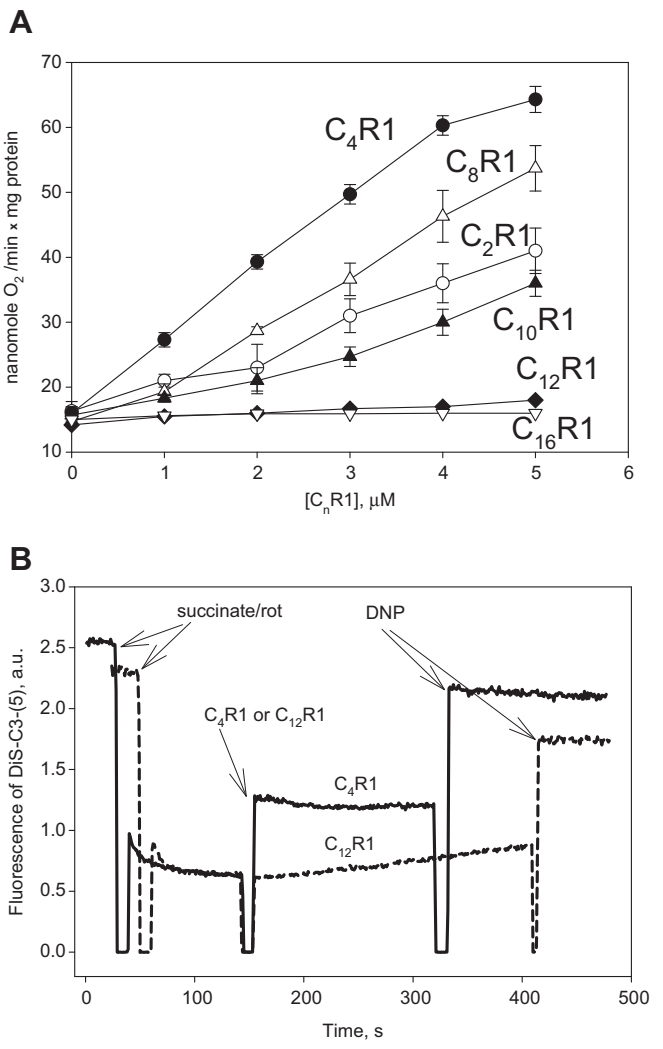

Fig. 3. A. Dose dependence of stimulation of the State 4 respiration by different derivatives of Rhodamine 19. Substrate, succinate. Other conditions are the same as in the legend to Fig. 1. B. Effect of C_4R1 and $C_{12}R1$ on the membrane potential of rat liver mitochondria measured by DiSC3-(5). Traces of fluorescence are shown using the medium described in "Materials and methods". Additions where indicated: 5 mM succinate + 1 μM rotenone, 2 μM C_4R1 or $C_{12}R1$, and 50 μM of DNP.

(59 mV at ΔpH = 1). $C_{12}R1$ induced electrical conductance through the BLM (see also [35]) that was several-folds higher than the conductance in the presence of C_4R1 (data not shown). Thus, the BLM experiments confirmed the conclusion of our previous data on liposomes [17] that the protonophorous action of C_4R1 on lipid membranes is weaker compared to that of $C_{12}R1$.

The inconsistency of the data on the relative efficacy of C_4R1 and $C_{12}R1$ on mitochondrial (Figs. 2,3) and artificial lipid (Fig. 4) membranes could be rationalized by the idea of the involvement of some mitochondrial membrane protein in the process of C_4R1-mediated uncoupling, similarly to participation of the ADP/ATP and aspartate/glutamate antiporters in the fatty acid-mediated uncoupling [21,36]. Our experiments showed that the inhibitor of the ADP/ATP carrier, carboxyatractyloside, did not inhibit C_4R1-mediated respiration (data not shown), although it has been found earlier that C_2R1 is able to inhibit the ADP/ATP carrier at low nucleotide concentrations [37]. We also tested the following inhibitors of: calcium uniporter (ruthenium red), Na^+/H^+-antiporter (amiloride), Complex I (rotenone), H^+-ATPase (DCCD and oligomycin). Moreover, we also tried 6-ketocholestanol, which inhibits the action of such potent uncouplers as SF6847 and FCCP [38]. All these inhibitors had no effect on the C_4R1-induced stimulation of State 4 respiration. Hence, the putative "C_4R1-carrier" is outside our list of candidates or, as in the case of fatty acids, several carriers are involved.

If C_4R1 interacts with a protein located in the matrix or in the inner mitochondrial membrane, its action must depend on C_4R1 accumulation in mitochondria, being maximal in the energized state. It has previously been shown that, in contrast to tetramethylrhodamine ethyl ester (TMRE), whose accumulation is strongly potential-dependent in cells and isolated mitochondria, uptake of $C_{12}R1$ by isolated mitochondria is rather significant even in the de-energized state [39]. Apparently,

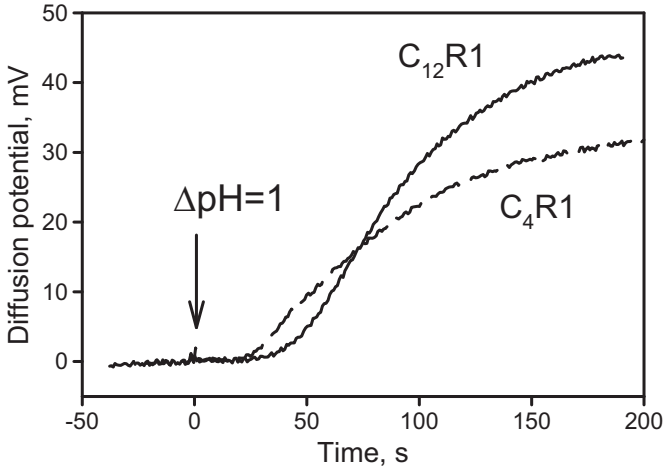

Fig. 4. Formation of $C_{12}R1$- or C_4R1-mediated H^+ diffusion potential on a planar bilayer phospholipid membrane. The solution contained 10 mM Tris and 100 mM KCl, pH 7.4. The BLM was made from total lipids of *E. coli*, and the concentration of $C_{12}R1$ or C_4R1 was 1.0 μM. Arrow, the pH in one of the BLM-separated compartments was shifted to 8.4 by adding KOH.

this is a result of the high lipophilicity of $C_{12}R1$. In the present work, we compared the energy-dependent uptake by mitochondria of C_4R1 and $C_{12}R1$ with that of TMRE, using fluorescence correlation spectroscopy as described previously [39]. Fig. S2 shows that C_4R1, similarly to TMRE and in contrast to $C_{12}R1$, showed a pronounced component of energy-dependent uptake. To further analyze the role of $\Delta\psi$ in the uptake of C_4R1 by mitochondria, we measured its protonophorous activity in non-energized mitochondria. The method of the measurements of mitochondrial swelling in a medium containing potassium acetate and valinomycin is suitable for addressing this question. It was previously shown that fatty acids are able to promote this type of swelling, in agreement with their ability to uncouple mitochondria in a de-energized state [26]. By contrast, low C_4R1 concentrations were unable to induce swelling of mitochondria under these conditions, while $C_{12}R1$ was active in this respect (Fig. 5A). These results combined with the data on uncoupling under energized conditions correlated well with the dependence of the potential-dependent accumulation of C_4R1 and $C_{12}R1$ in mitochondria (Fig. S2). Importantly, increasing the extramitochondrial concentration of C_4R1 from 1 to 50 μM led to induction of mitochondria swelling comparable to that induced by FCCP even in non-energized mitochondria (Fig. 5B), a fact confirming the assumption that $\Delta\psi$ was needed to accumulate C_4R1 inside mitochondria. It should be stressed that 50 μM C_4R1 operated as a protonophore rather than a detergent because its effect on swelling was valinomycin-dependent (Fig. 5B).

Fig. 6 shows the effect of C_4R1, $C_{12}R1$, and FCCP on respiration of suspended HeLa cells. The respiration was strongly inhibited by oligomycin, indicating high activity of oxidative phosphorylation in the cells. In the presence of oligomycin, the respiration was rapidly stimulated by nanomolar concentrations of C_4R1 and reached saturation at about 1.5 μM (Fig. 6A). Interestingly, in the interval of C_4R1 concentrations from 50 nM to about 300 nM, the C_4R1-stimulated respiration remained sensitive to oligomycin, indicating that the oxidative phosphorylation was not blocked yet under these conditions (Fig. 6A). Fig. 6B shows the effect of $C_{12}R1$ on respiration of HeLa cells. In these experiments, the cells were pre-incubated for 2 h with $C_{12}R1$ prior to measurements in order to complete the accumulation of $C_{12}R1$. In the case of measuring the effect of $C_{12}R1$ on respiration without pre-incubation, the acting concentrations of $C_{12}R1$ were in the range of several micromolar, which was much larger than for C_4R1 (not shown). In experiments with $C_{12}R1$ pre-incubation, the acting concentrations of $C_{12}R1$ were in sub-micromolar range (Fig. 6B). At higher concentrations of $C_{12}R1$, the fully uncoupled (FCCP) respiration decreased, indicating

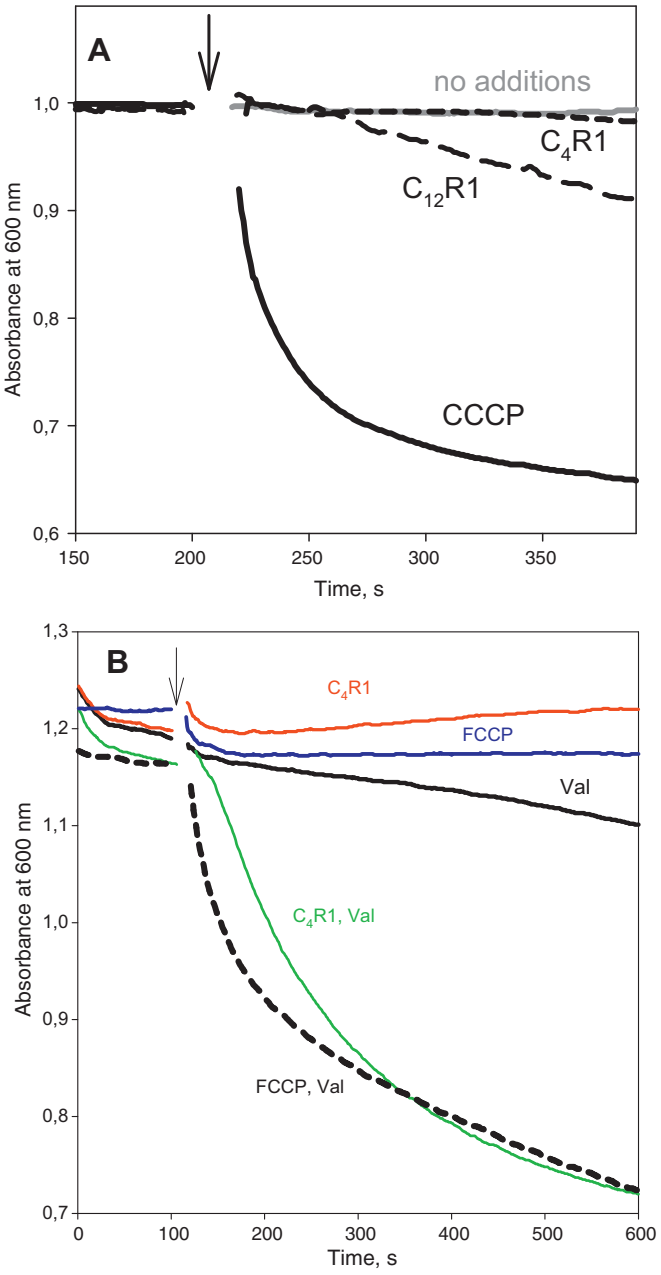

Fig. 5. Effect of $C_{12}R1$ and C_4R1 on the swelling of rat liver mitochondria in potassium acetate medium. Incubation mixture: 145 mM potassium acetate, 5 mM TRIS, 0.5 mM EDTA, pH 7.4, and 1 μM rotenone. Mitochondrial protein 0.5 mg/ml. Additions: 4 μM C_4R1 (A) or 50 μM C_4R1 (B), 4 μM $C_{12}R1$; 2 μM CCCP, 2 μM FCCP. In A, 1 μM valinomycin was present in all the cases. In B, it was added where indicated.

inhibition of the respiratory chain by $C_{12}R1$ (Fig. 6B). Fig. 6C displays the titration of HeLa cell respiration with FCCP.

In the next series of experiments, we analyzed accumulation of the rhodamine conjugates in HeLa cells. Flow cytometric measurements showed that C_4R1 accumulated in these cells faster than $C_{12}R1$ (Fig. 7). The uncoupler FCCP inhibited accumulation of both rhodamines. The release of C_4R1 from cells after replacing the rhodamine-containing medium by that without rhodamine was also faster in comparison with $C_{12}R1$ (Fig. 7). A significant fraction of $C_{12}R1$ (but not C_4R1) remained associated with cells even when FCCP was added after changing the medium (not shown). Imaging of C_4R1 accumulation in substrate-attached HeLa cells revealed its fast appearance in mitochondria, in contrast to $C_{12}R1$, which at first stained the plasma membrane and probably the other intracellular membranes (seen as a diffuse staining) (Fig. S3).

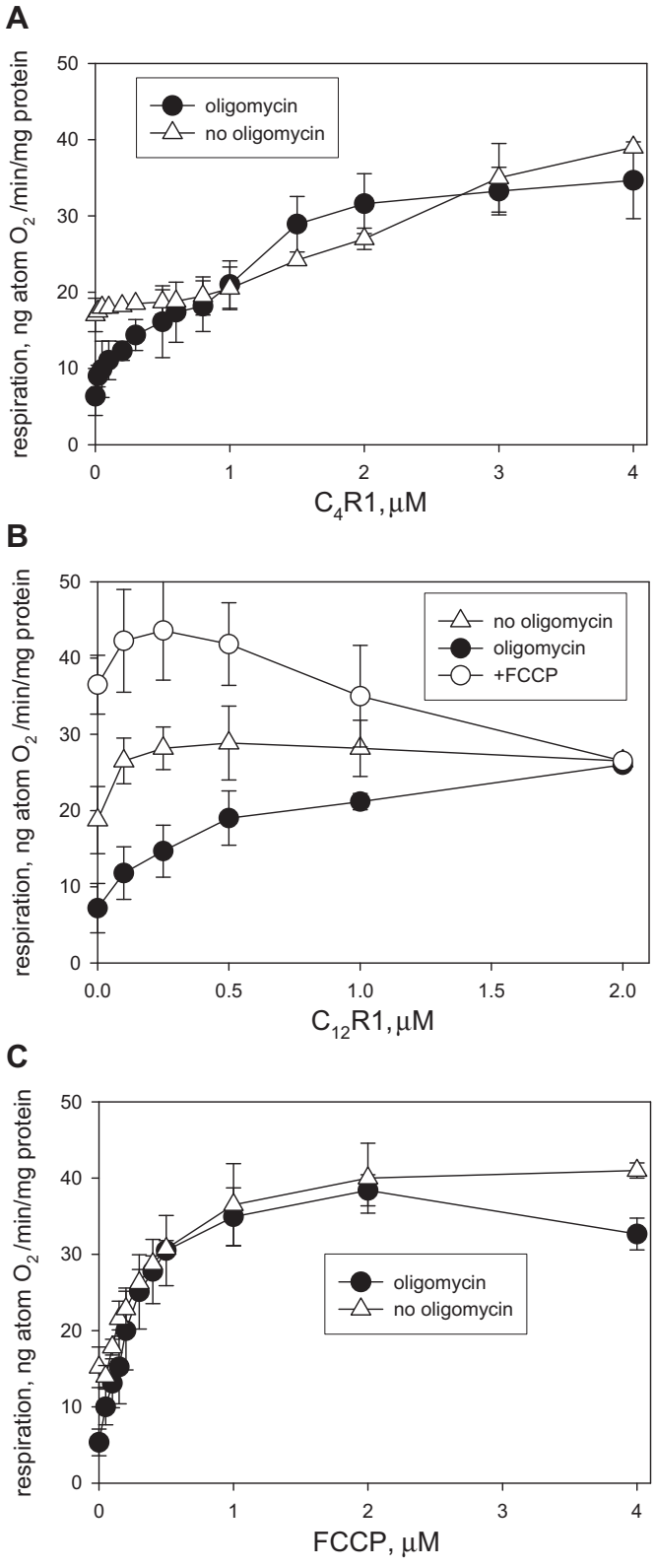

Fig. 6. Effects of C_4R1 (panel A), $C_{12}R1$ (panel B), and FCCP (panel C) on respiration of HeLa cells. C_4R1 was added to the cells and respiration rate was measured when the stationary respiration rate was established after 4–5 min. $C_{12}R1$ was added to the cell culture followed by incubation for 2 h, and respiration was analyzed after harvesting and washing of the cells. The final cell concentration in polarographic chamber was $4–5 \times 10^6$ cells/ml. Where indicated, oligomycin (10 μg/ml) or FCCP (2 μM) was added to the measuring chamber. Oxygen consumption was recorded at 37 °C.

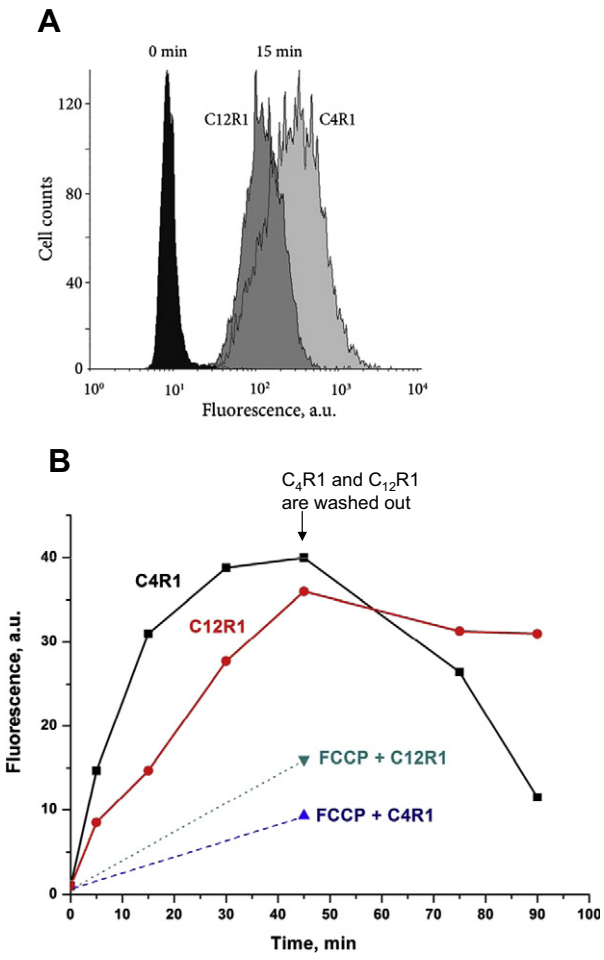

Fig. 7. Accumulation of C_4R1 or $C_{12}R1$ in HeLa cells measured by flow cytometry. A. Histograms of cell fluorescence immediately after the addition of rhodamine compounds and after 15 min incubation. **B**. Kinetics of the C_4R1 or $C_{12}R1$ accumulation. Cells were incubated with 100 nM C_4R1 or $C_{12}R1$. After 45 min, the Rhodamine compounds were washed out and measurements were continued. Where indicated, 10 μM FCCP was added 30 min before the Rhodamine compounds.

These observations apparently reflected lower lipophilicity of C_4R1 in comparison to $C_{12}R1$. After extended incubation, both compounds were selectively accumulated in mitochondria (Fig. S3, 30 min images).

The obvious advantage of the rhodamines is their bright fluorescence, which allows identifying their tissue localization. Fig. S4 shows examples of brain and kidney slices imaged 3 h after i/p injection of C_4R1. The kidney slices exhibited bright fluorescence of C_4R1 (Fig. S4A, B), while only limited staining of brain blood vessels was seen in the case of brain slices (Fig. S4C, D). We conclude that C_4R1 permeates through the brain–blood barrier rather slowly. In this context, it seems remarkable that the neuroprotective action of SkQR1 was shown to be partially mediated via synthesis of erythropoietin in kidney [40].

4. Discussion

Similarly to TMRE and mitochondria-targeted antioxidants (MitoQ, SkQ), cationic C_4R1 electrophoretically accumulates inside mitochondria (organelle interior negative). This accumulation must substantially increase the biological efficiency of these compounds. Moreover, the effect of any cationic uncouplers should strongly depend on membrane potential, exhibiting self-limitation of the uncoupling action because the membrane potential is the driving force for accumulation of these uncouplers in mitochondria, but, when accumulated, the uncouplers lower membrane potential responsible for the accumulation. Consistent

with this statement, low concentrations of C_4R1 had no effect on the proton permeability of mitochondria in their non-energized state as assessed by swelling in potassium acetate in the presence of valinomycin (Fig. 5). With respect to $\Delta\psi$ dependence, uncoupling by C_4R1 resembles that exerted by a natural uncoupler, UCP1, which shows high H^+ conductance only at membrane potential above some threshold [41]. Inability of low C_4R1 concentrations to induce H^+ conductance in lipid membranes can most probably be related to its poor binding to the membrane.

A general scheme of the operation of C_4R1 as an inducer of H^+ conductance in mitochondria might be the following. (1) C_4R1 accumulates electrophoretically in the interior of mitochondria. (2) Accumulation of C_4R1 inside mitochondria results in saturation of the inner mitochondrial membrane with C_4R1, including the binding of C_4R1 to inner membrane protein(s) that facilitate transmembrane movement of protonated (cationic) form, which is the rate-limiting step. (3) Electroneutral (deprotonated) C_4R1 crosses the membrane in a protein-independent manner. This hypothesis explains the essential features of the C_4R1-mediated uncoupling phenomenon: (a) lower efficiency of small C_4R1 concentrations in the bilayer lipid membrane (where no proteins are present), (b) requirement of energization of mitochondria to create H^+-conductance (which is necessary to accumulate C_4R1 inside mitochondria), (c) inefficiency of C_4R4 (lacking ionizable H^+), and (d) in mitochondria, higher efficiency of C_4R1 compared to $C_{12}R1$, the latter being assumed to be unable to be recognized by the protein carriers. The identification of these putative mitochondrial proteins is a task of our future work.

Limited uncoupling induced by low doses of uncouplers was shown to lead to favorable therapeutic action in a number of laboratory animal models [2]. It was suggested that certain pathological processes in neurons proceed via the induction of nonspecific permeability of mitochondria and the accumulation of high levels of Ca^{2+} associated with excessive generation of ROS [42–44], which can lead to either apoptotic or necrotic cell death [45]. In our experiments, we have demonstrated that treatment with mitochondria-targeted uncouplers resulted in a significant reduction in the brain damage and swelling as well as better behavioral outcomes than measured in vehicle-treated animals. These results highlight the importance of early adverse mitochondrial events in brain damage during ischemia/reperfusion and support the concept that "mild" mitochondrial uncoupling may be an important neuroprotective strategy for the treatment of stroke and other brain pathologies associated with cellular oxidative stress. C_4R1 and $C_{12}R1$ exhibited similar protective action on the volume of ischemic damage, while C_4R1 was substantially more active than $C_{12}R1$ in the reduction of brain swelling and brain function distortion. Some uncoupling activity of $C_{12}R1$ can be explained by proton cycling without assistance of any protein and/or by translocation of anions of fatty acids [46].

As previously demonstrated, the classical uncouplers DNP and FCCP are neuroprotectors. Using the model of Parkinson's disease studied on slices of rat brain, it has been shown that DNP and FCCP significantly antagonized and delayed the ability of rotenone to potentiate ion currents evoked by N-methyl-D-aspartate [47]. In a study by Pandya et al., DNP and FCCP were used at an optimal dose of 5 and 2.5 mg/kg, correspondingly, after intervention 5-min-post-injury on the model of trauma. They found that these substances improve brain mitochondrial function and neurological outcomes [48,49]. Similar results were obtained for DNP used after post-reperfusion administration with the stroke model [16]. The neuroprotective efficacy of DNP was confirmed in a chemical model of neurodegeneration [50]. Unfortunately, DNP has a very narrow therapeutic window, since in rodents the toxic concentrations of DNP exceeded therapeutic concentration by only 2-3-fold [50,51]. DNP was widely used in clinical practice for weight loss in the beginning of the 20th century, but it was banned for the market by the FDA due to several deaths caused by side-effects associated with overdosing and severe uncoupling of mitochondria [52]. C_4R1, as a self-limiting uncoupler, may be a stepping-stone to creation of an artificial inducer of a UCP1-like "mild" uncoupling with a therapeutic window much larger than the classical (anionic) protonophores.

Acknowledgment

The authors thank Dr. Elena Kotova and Dr. Lev Yaguzhinsky for valuable comments and Dr. Elena Omarova for technical assistance. This work was supported in part by the Russian Foundation for Basic Research grants 12-04-00199,13-04-01530, 12-04-31970, 14-04-00300, and 14-94-00542 and the Institute of Mitoengineering, Moscow State University. RSF grants 14-15-00107, 14-15-00147, 14-24-00107 and Grant of the President of Russia MK-2508.2014.4.

Appendix A. Supplementary data

Supplementary data to this article can be found online at http://dx.doi.org/10.1016/j.bbabio.2014.07.006.

References

[1] V.P. Skulachev, Role of uncoupled and non coupled oxidations in maintenance of safely low levels of oxygen and its one electron reductants, Q. Rev. Biophys. 29 (1996) 169–202.
[2] F.M. Cunha, C.C. Caldeira da Silva, F.M. Cerqueira, A.J. Kowaltowski, Mild mitochondrial uncoupling as a therapeutic strategy, Curr. Drug Targets 12 (6) (2011) 783–789.
[3] G. Kaim, P. Dimroth, ATP synthesis by F-type ATP synthase is obligatorily dependent on the transmembrane voltage, EMBO J. 18 (1999) 4118–4127.
[4] B. Kadenbach, R. Ramzan, L. Wen, S. Vogt, New extension of the Mitchell Theory for oxidative phosphorylation in mitochondria of living organisms, Biochim. Biophys. Acta 1800 (2010) 205–212.
[5] S. Arnold, Cytochrome c oxidase and its role in neurodegeneration and neuroprotection, Adv. Exp. Med. Biol. 748 (2012) 305–339.
[6] S.S. Korshunov, V.P. Skulachev, A.A. Starkov, High protonic potential actuates a mechanism of production of reactive oxygen species in mitochondria, FEBS Lett. 416 (1997) 15–18.
[7] A.A. Starkov, G. Fiskum, Regulation of brain mitochondrial H2O2 production by membrane potential and NAD(P)H redox state, J. Neurochem. 86 (2003) 1101–1107.
[8] V.P. Skulachev, Membrane-linked systems preventing superoxide formation, Biosci. Rep. 17 (1997) 347–366.
[9] R.G. Hansford, B.A. Hogue, V. Mildaziene, Dependence of H_2O_2 formation by rat heart mitochondria on substrate availability and donor age, J. Bioenerg. Biomembr. 29 (1997) 89–95.
[10] V.P. Skulachev, Uncoupling: new approaches to an old problem of bioenergetics, Biochim. Biophys. Acta 1363 (1998) 100–124.
[11] P.G. Sullivan, C. Dube, K. Dorenbos, O. Steward, T.Z. Baram, Mitochondrial uncoupling protein-2 protects the immature brain from excitotoxic neuronal death, Ann. Neurol. 53 (2003) 711–717.
[12] P.G. Sullivan, J.E. Springer, E.D. Hall, S.W. Scheff, Mitochondrial uncoupling as a therapeutic target following neuronal injury, J. Bioenerg. Biomembr. 36 (2004) 353–356.
[13] G. Mattiasson, M. Shamloo, G. Gido, K. Mathi, G. Tomasevic, S. Yi, C.H. Warden, R.F. Castilho, T. Melcher, M. Gonzalez-Zulueta, K. Nikolich, T. Wieloch, Uncoupling protein-2 prevents neuronal death and diminishes brain dysfunction after stroke and brain trauma, Nat. Med. 9 (2003) 1062–1068.
[14] B. Conti, S. Sugama, J. Lucero, R. Winsky-Sommerer, S.A. Wirz, P. Maher, Z. Andrews, A.M. Barr, M.C. Morale, C. Paneda, J. Pemberton, S. Gaidarova, M.M. Behrens, F. Beal, P.P. Sanna, T. Horvath, T. Bartfai, Uncoupling protein 2 protects dopaminergic neurons from acute 1,2,3,6-methyl-phenyl-tetrahydropyridine toxicity, J. Neurochem. 93 (2005) 493–501.
[15] M.R. Duchen, Mitochondria, calcium-dependent neuronal death and neurodegenerative disease, Pflugers Arch. 464 (2012) 111–121.
[16] A.S. Korde, P.G. Sullivan, W.F. Maragos, The uncoupling agent 2,4-dinitrophenol improves mitochondrial homeostasis following striatal quinolinic acid injections, J. Neurotrauma 22 (2005) 1142–1149.
[17] Y.N. Antonenko, A.V. Avetisyan, D.A. Cherepanov, D.A. Knorre, G.A. Korshunova, O.V. Markova, S.M. Ojovan, I.V. Perevoshchikova, A.V. Pustovidko, T.I. Rokitskaya, I.I. Severina, R.A. Simonyan, E.A. Smirnova, A.A. Sobko, N.V. Sumbatyan, F.F. Severin, V.P. Skulachev, Derivatives of rhodamine 19 as mild mitochondria-targeted cationic uncouplers, J. Biol. Chem. 286 (2011) 17831–17840.
[18] A.Y. Andreyev, T.O. Bondareva, V.I. Dedukhova, E.N. Mokhova, V.P. Skulachev, L.M. Tsofina, N.I. Volkov, T.V. Vygodina, The ATP/ADP-antiporter is involved in the uncoupling effect of fatty acids on mitochondria, Eur. J. Biochem. 182 (1989) 585–592.
[19] E.Y. Plotnikov, D.N. Silachev, S.S. Jankauskas, T.I. Rokitskaya, A.A. Chupyrkina, I.B. Pevzner, L.D. Zorova, N.K. Isaev, Y.N. Antonenko, V.P. Skulachev, D.B. Zorov, Mild uncoupling of respiration and phosphorylation as a mechanism providing nephro- and neuroprotective effects of penetrating cations of the SkQ family, Biochemistry (Mosc) 77 (2012) 1029–1037.
[20] P.H. Lou, B.S. Hansen, P.H. Olsen, S. Tullin, M.P. Murphy, M.D. Brand, Mitochondrial uncouplers with an extraordinary dynamic range, Biochem. J. 407 (2007) 129–140.

[21] V.P. Skulachev, Uncoupling: new approaches to an old problem of bioenergetics, Biochim. Biophys. Acta 1363 (1998) 100–124.
[22] Y.N. Antonenko, A.V. Avetisyan, L.E. Bakeeva, B.V. Chernyak, V.A. Chertkov, L.V. Domnina, O.Y. Ivanova, D.S. Izyumov, L.S. Khailova, S.S. Klishin, G.A. Korshunova, K.G. Lyamzaev, M.S. Muntyan, O.K. Nepryakhina, A.A. Pashkovskaya, O.Y. Pletjushkina, A.V. Pustovidko, V.A. Roginsky, T.I. Rokitskaya, E.K. Ruuge, V.B. Saprunova, I.I. Severina, R.A. Simonyan, I.V. Skulachev, M.V. Skulachev, N.V. Sumbatyan, I.V. Sviryaeva, V.N. Tashlitsky, J.M. Vassiliev, M.Y. Vyssokikh, L.S. Yaguzhinsky, A.A. Zamyatnin Jr., V.P. Skulachev, Mitochondria-targeted plastoquinone derivatives as tools to interrupt execution of the aging program. 1. Cationic plastoquinone derivatives: synthesis and in vitro studies, Biochemistry (Mosc) 73 (2008) 1273–1287.
[23] T.I. Rokitskaya, N.V. Sumbatyan, V.N. Tashlitsky, G.A. Korshunova, Y.N. Antonenko, V.P. Skulachev, Mitochondria-targeted penetrating cations as carriers of hydrophobic anions through lipid membranes, Biochim. Biophys. Acta 1798 (2010) 1698–1706.
[24] D. Johnson, H. Lardy, Isolation of liver or kidney mitochondria, Methods Enzymol. 10 (1967) 94–96.
[25] P.C. Laris, D.P. Bahr, R.R. Chaffee, Membrane potentials in mitochondrial preparations as measured by means of a cyanine dye, Biochim. Biophys. Acta 376 (1975) 415–425.
[26] P. Schonfeld, M.R. Wieckowski, L. Wojtczak, Long-chain fatty acid-promoted swelling of mitochondria: further evidence for the protonophoric effect of fatty acids in the inner mitochondrial membrane, FEBS Lett. 471 (2000) 108–112.
[27] K.D. Garlid, R.A. Nakashima, Studies on the mechanism of uncoupling by amine local anesthetics. Evidence for mitochondrial proton transport mediated by lipophilic ion pairs, J. Biol. Chem. 258 (1983) 7974–7980.
[28] I.V. Perevoshchikova, D.B. Zorov, Y.N. Antonenko, Peak intensity analysis as a method for estimation of fluorescent probe binding to artificial and natural nanoparticles: tetramethylrhodamine uptake by isolated mitochondria, Biochim. Biophys. Acta 1778 (2008) 2182–2190.
[29] D.N. Silachev, A.A. Uchevatkin, Y.A. Pirogov, D.B. Zorov, N.K. Isaev, Comparative evaluation of two methods for studies of experimental focal ischemia: magnetic resonance tomography and triphenyltetrazoleum detection of brain injuries, Bull. Exp. Biol. Med. 147 (2009) 269–272.
[30] F.C. Barone, R.K. Clark, G. Feuerstein, R.E. Lenkinski, S.K. Sarkar, Quantitative comparison of magnetic resonance imaging (MRI) and histologic analyses of focal ischemic damage in the rat, Brain Res. Bull. 26 (1991) 285–291.
[31] J. Jolkkonen, K. Puurunen, S. Rantakomi, A. Harkonen, A. Haapalinna, J. Sivenius, Behavioral effects of the alpha(2)-adrenoceptor antagonist, atipamezole, after focal cerebral ischemia in rats, Eur. J. Pharmacol. 400 (2000) 211–219.
[32] J.O. Strom, E. Ingberg, A. Theodorsson, E. Theodorsson, Method parameters' impact on mortality and variability in rat stroke experiments: a meta-analysis, BMC Neurosci. 14 (2013) 41.
[33] V.P. Skulachev, A.A. Sharaf, L.S. Yagujzinsky, A.A. Jasaitis, E.A. Liberman, V.P. Topali, The effect of uncouplers on mitochondria, respiratory enzyme complexes and artificial phospholipid membranes, Curr. Mod. Biol. 2 (1968) 98–105.
[34] L.S. Yaguzhinsky, E.G. Smirnova, L.A. Ratnikova, G.M. Kolesova, I.P. Krasinskaya, Hydrophobic sites of the mitochondrial electron transfer system, J. Bioenerg. Biomembr. 5 (1) (1973) 163–174.
[35] T.I. Rokitskaya, T.M. Ilyasova, I.I. Severina, Y.N. Antonenko, V.P. Skulachev, Electrogenic proton transport across lipid bilayer membranes mediated by cationic derivatives of rhodamine 19: comparison with anionic protonophores, Eur. Biophys. J. 42 (2013) 477–485.
[36] P. Jezek, H. Engstova, M. Zackova, A.E. Vercesi, A.D. Costa, P. Arruda, K.D. Garlid, Fatty acid cycling mechanism and mitochondrial uncoupling proteins, Biochim. Biophys. Acta 1365 (1998) 319–327.
[37] A.R. Gear, Rhodamine 6G. A potent inhibitor of mitochondrial oxidative phosphorylation, J. Biol. Chem. 249 (1974) 3628–3637.
[38] A.A. Starkov, V.I. Dedukhova, V.P. Skulachev, 6-Ketocholestanol abolishes the effect of the most potent uncouplers of oxidative phosphorylation in mitochondria, FEBS Lett. 355 (1994) 305–308.
[39] Y.N. Antonenko, I.V. Perevoshchikova, T.I. Rokitskaya, R.A. Simonyan, V.V. Tashlitsky, V.P. Skulachev, Effect of liposomes on energy-dependent uptake of the antioxidant SkQR1 by isolated mitochondria, J. Bioenerg. Biomembr. 44 (2012) 453–460.
[40] D.N. Silachev, N.K. Isaev, I.B. Pevzner, L.D. Zorova, E.V. Stelmashook, S.V. Novikova, E.Y. Plotnikov, V.P. Skulachev, D.B. Zorov, The mitochondria-targeted antioxidants and remote kidney preconditioning ameliorate brain damage through kidney-to-brain cross-talk, PLoS ONE 7 (2012) e51553.
[41] A. Rupprecht, E.A. Sokolenko, V. Beck, O. Ninnemann, M. Jaburek, T. Trimbuch, S.S. Klishin, P. Jezek, V.P. Skulachev, E.E. Pohl, Role of the transmembrane potential in the membrane proton leak, Biophys. J. 98 (2010) 1503–1511.
[42] C. Martel, I.H. Huynh, A. Garnier, R. Ventura-Clapier, C. Brenner, Inhibition of the mitochondrial permeability transition for cytoprotection: direct versus indirect mechanisms, Biochem. Res. Int. (2012) 213403.
[43] S.G. Carriedo, H.Z. Yin, S.L. Sensi, J.H. Weiss, Rapid Ca^{2+} entry through Ca^{2+}-permeable AMPA/Kainate channels triggers marked intracellular Ca^{2+} rises and consequent oxygen radical production, J. Neurosci. 18 (1998) 7727–7738.
[44] L.L. Dugan, S.L. Sensi, L.M. Canzoniero, S.D. Handran, S.M. Rothman, T.S. Lin, M.P. Goldberg, D.W. Choi, Mitochondrial production of reactive oxygen species in cortical neurons following exposure to N-methyl-D-aspartate, J. Neurosci. 15 (1995) 6377–6388.
[45] M. Ankarcrona, J.M. Dypbukt, E. Bonfoco, B. Zhivotovsky, S. Orrenius, S.A. Lipton, P. Nicotera, Glutamate-induced neuronal death: a succession of necrosis or apoptosis depending on mitochondrial function, Neuron 15 (1995) 961–973.
[46] F.F. Severin, I.I. Severina, Y.N. Antonenko, T.I. Rokitskaya, D.A. Cherepanov, E.N. Mokhova, M.Y. Vyssokikh, A.V. Pustovidko, O.V. Markova, L.S. Yaguzhinsky, G.A. Korshunova, N.V. Sumbatyan, M.V. Skulachev, V.P. Skulachev, Penetrating cation/fatty acid anion pair as a mitochondria-targeted protonophore, Proc. Natl. Acad. Sci. U. S. A. 107 (2010) 663–668.
[47] Y.N. Wu, A.C. Munhall, S.W. Johnson, Mitochondrial uncoupling agents antagonize rotenone actions in rat substantia nigra dopamine neurons, Brain Res. 1395 (2011) 86–93.
[48] J.D. Pandya, J.R. Pauly, P.G. Sullivan, The optimal dosage and window of opportunity to maintain mitochondrial homeostasis following traumatic brain injury using the uncoupler FCCP, Exp. Neurol. 218 (2009) 381–389.
[49] J.D. Pandya, J.R. Pauly, V.N. Nukala, A.H. Sebastian, K.M. Day, A.S. Korde, W.F. Maragos, E.D. Hall, P.G. Sullivan, Post-injury administration of mitochondrial uncouplers increases tissue sparing and improves behavioral outcome following traumatic brain injury in rodents, J. Neurotrauma 24 (2007) 798–811.
[50] W.F. Maragos, K.T. Rockich, J.J. Dean, K.L. Young, Pre- or post-treatment with the mitochondrial uncoupler 2,4-dinitrophenol attenuates striatal quinolinate lesions, Brain Res. 966 (2003) 312–316.
[51] J.A. Harper, K. Dickinson, M.D. Brand, Mitochondrial uncoupling as a target for drug development for the treatment of obesity, Obes. Rev. 2 (2001) 255–265.
[52] J. Grundlingh, P.I. Dargan, M. El Zanfaly, D.M. Wood, 2,4-Dinitrophenol (DNP): a weight loss agent with significant acute toxicity and risk of death, J. Med. Toxicol. 7 (2011) 205–212.